

Supporting information

Bimetallic Ni-Co Selenides Heterostructure Aerogel for High-efficient Overall Water Splitting

Hongchen Liu, Fan Yang*, Fengjiang Chen, Sai Che, Neng Chen, Chong Xu, Ni Wu,
Wenkai Wei and Yongfeng Li

State Key Laboratory of Heavy Oil Processing, China University of Petroleum,
Beijing, Changping 102249, China

E-mail: yangfan@cup.edu.cn (F. Yang); yfli@cup.edu.cn (Y.F. Li)

* Corresponding authors' E-mail: yangfan@cup.edu.cn (F. Yang), Tel: +86-10-89733897;

* Corresponding authors' E-mail: yfli@cup.edu.cn (Y.F. Li), Tel: +86-10-89733897.

Figure S1

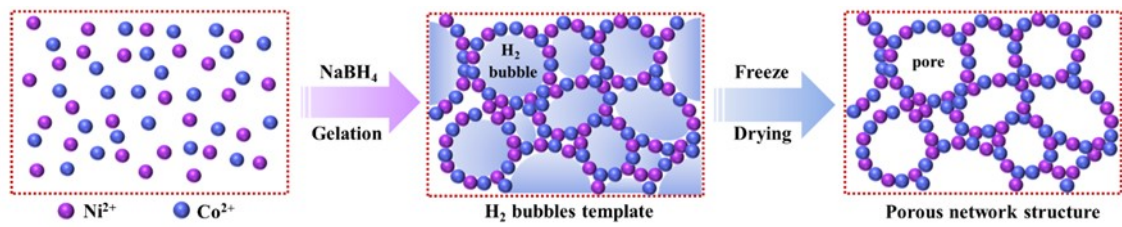


Figure S1. Schematic illustration for the generation of porous network structure.

Figure S2

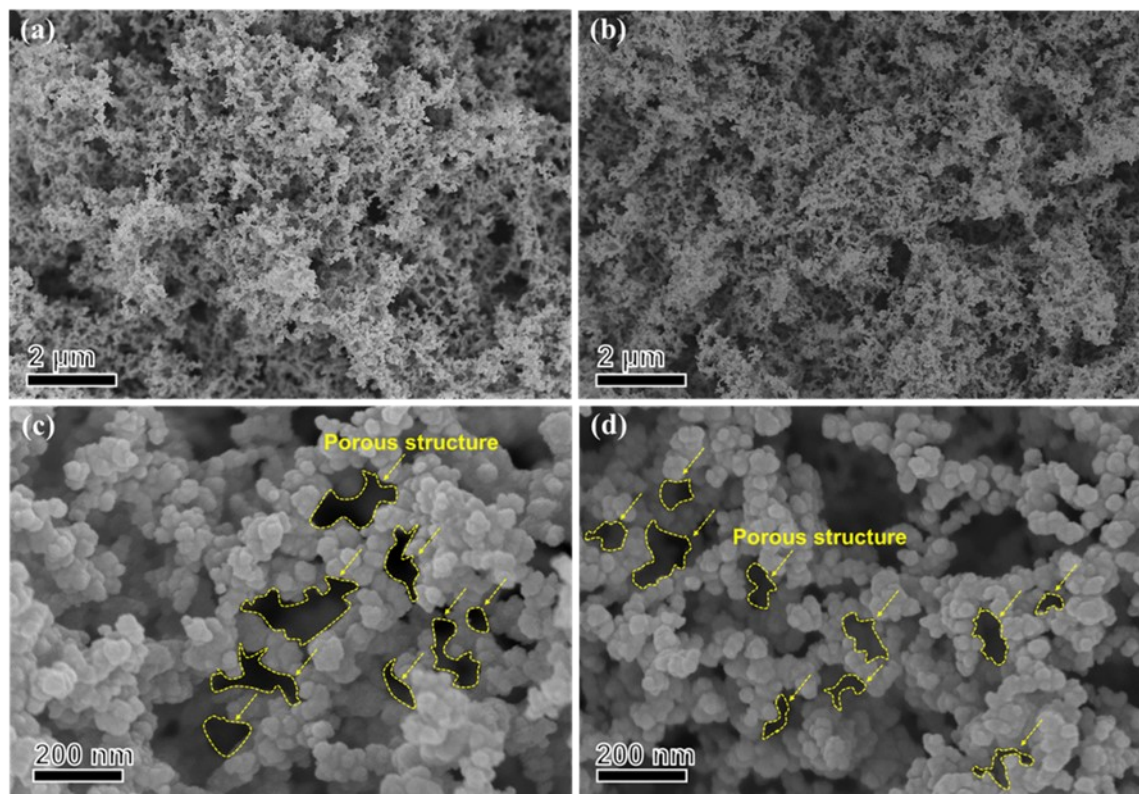


Figure S2. (a-b) Low-resolution SEM images of Ni-Co and NiSe₂-CoSe₂ aerogels. (c-d) High-resolution SEM images of Ni-Co and NiSe₂-CoSe₂ aerogels.

Figure S3

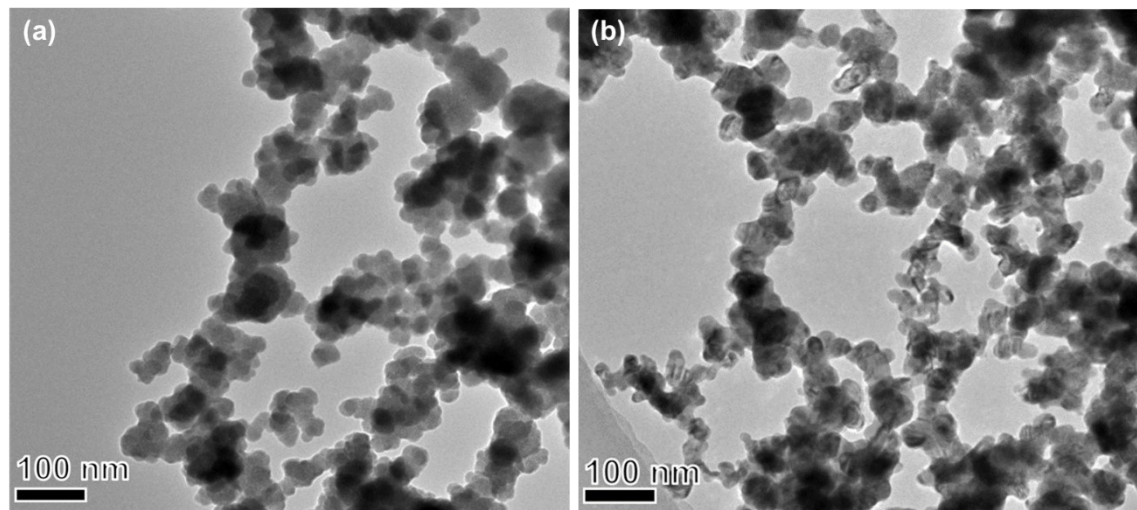


Figure S3. (a) TEM image of Ni-Co aerogel. (b) TEM image of $\text{NiSe}_2\text{-CoSe}_2$ aerogel.

Figure S4

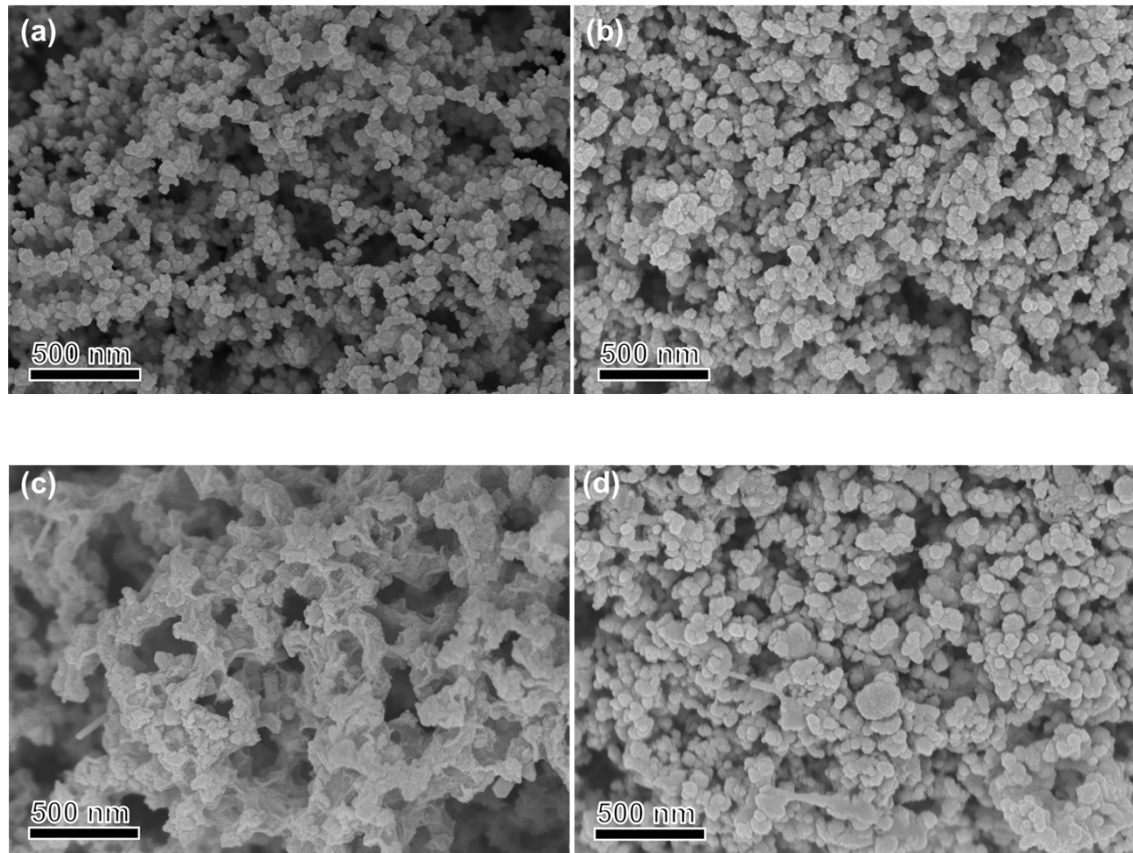


Figure S4. (a) SEM image of NiSe₂-CoSe₂-2:1 aerogel. (b) SEM image of NiSe₂-CoSe₂-1:2 aerogel. (c) SEM image of NiSe₂ aerogel. (d) SEM image of CoSe₂ aerogel.

Figure S5

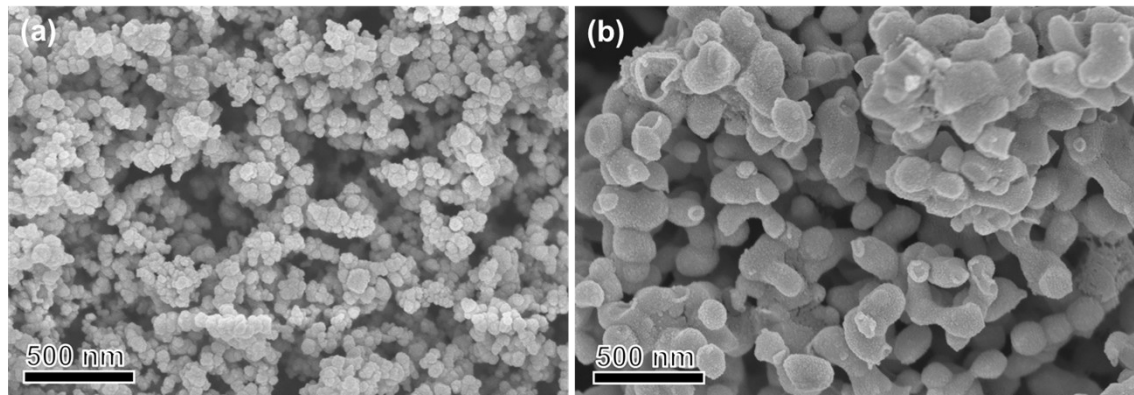


Figure S5. (a) SEM image of $\text{NiSe}_2\text{-CoSe}_2\text{-300}$ aerogel. (b) SEM image of $\text{NiSe}_2\text{-CoSe}_2\text{-500}$ aerogel.

Figure S6

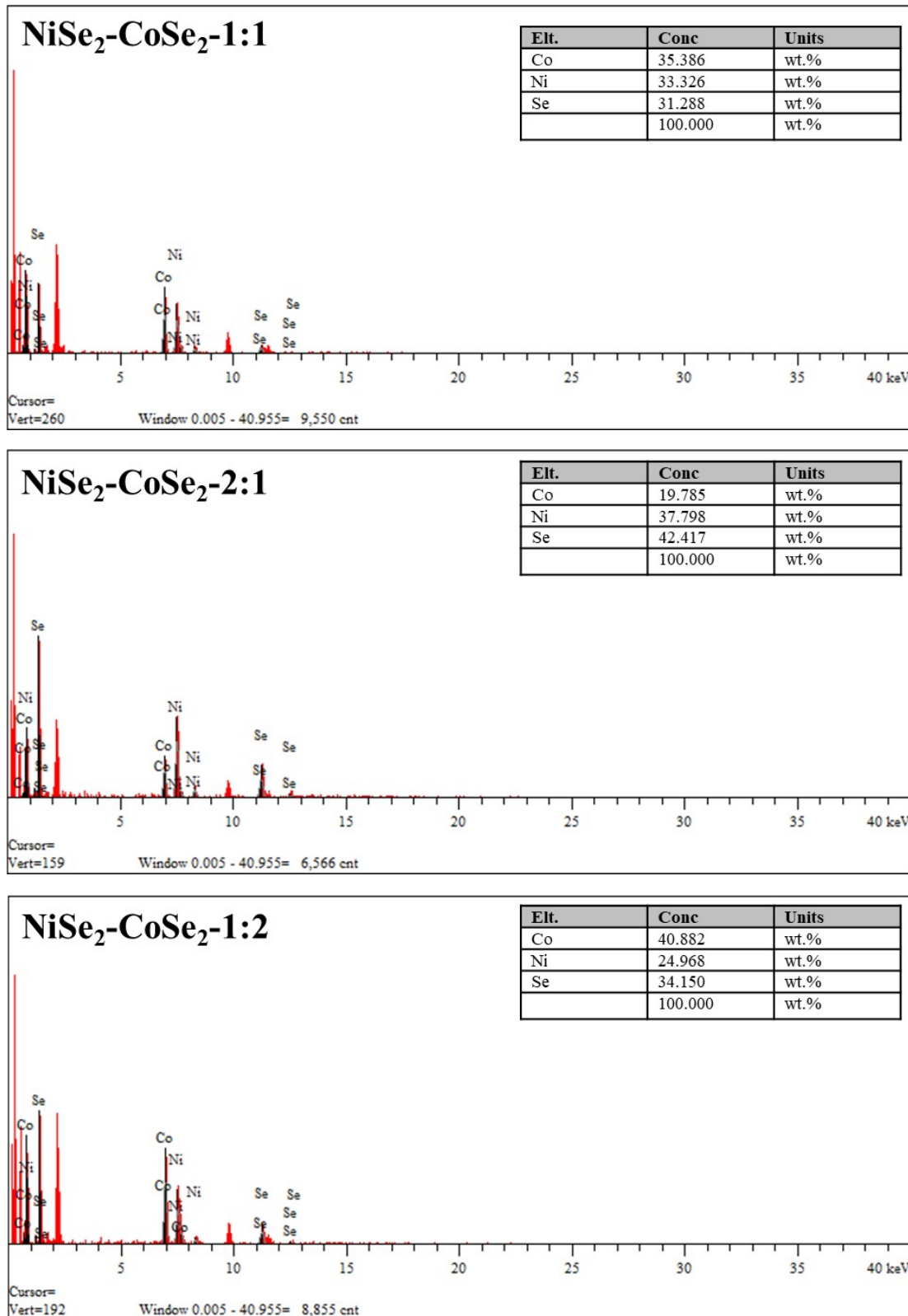


Figure S6. SEM-EDS of NiSe₂-CoSe₂-1:1, NiSe₂-CoSe₂-2:1 and NiSe₂-CoSe₂-1:2 aerogels.

Figure S7

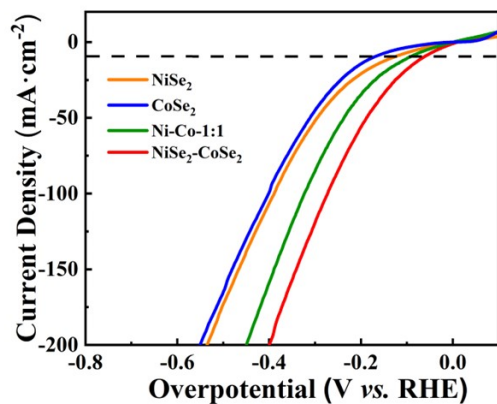


Figure S7. Polarization LSV curves without IR-correction of NiSe₂, CoSe₂, Ni-Co, and NiSe₂-CoSe₂ aerogels toward HER in 1.0M KOH.

Figure S8

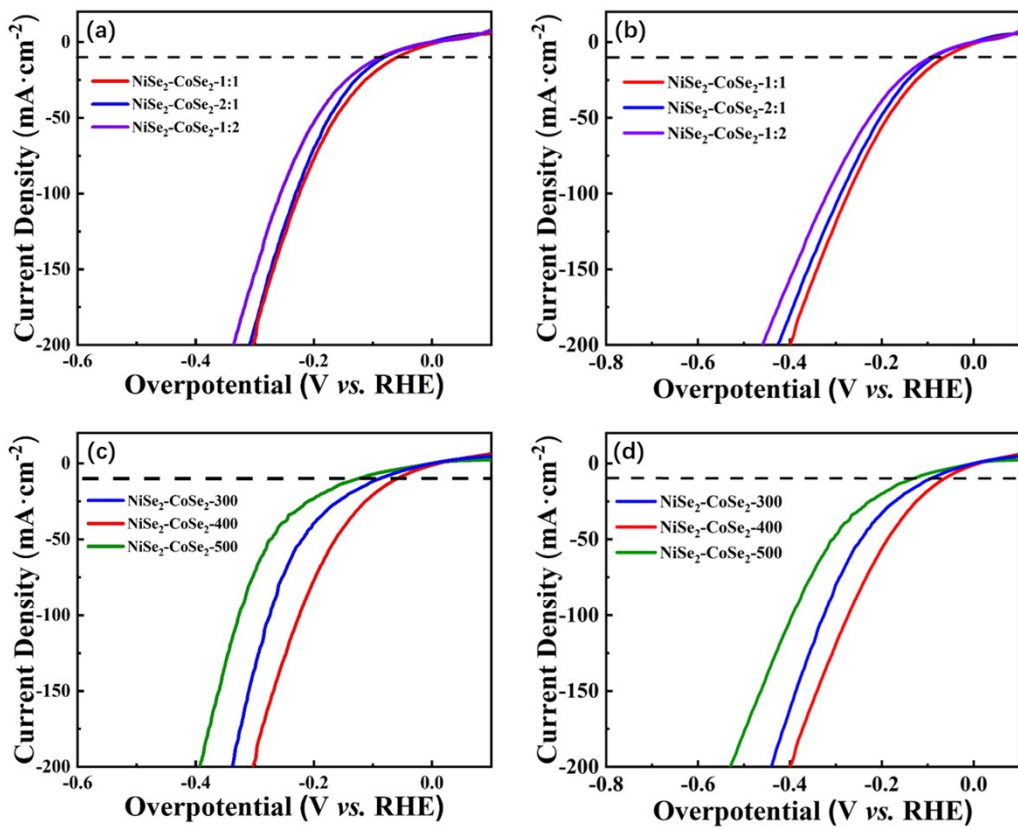


Figure S8. (a-b) Polarization LSV curves of $\text{NiSe}_2\text{-CoSe}_2$ -1:1, $\text{NiSe}_2\text{-CoSe}_2$ -2:1 and $\text{NiSe}_2\text{-CoSe}_2$ -1:2 aerogels toward HER in 1.0M KOH (with and without IR-correction). (c-d) Polarization LSV curves of $\text{NiSe}_2\text{-CoSe}_2$ -300, $\text{NiSe}_2\text{-CoSe}_2$ -400 and $\text{NiSe}_2\text{-CoSe}_2$ -500 aerogels toward HER in 1.0M KOH (with and without IR-correction).

Figure S9

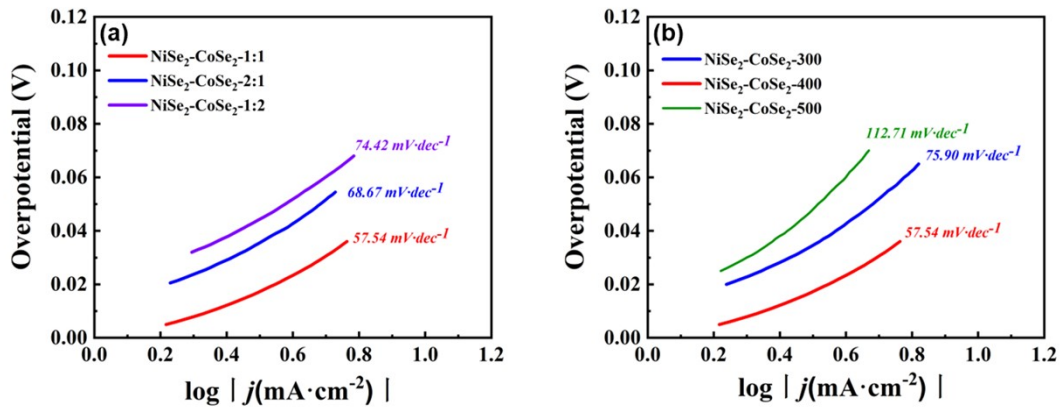


Figure S9. (a) Tafel slopes of NiSe₂-CoSe₂-1:1, NiSe₂-CoSe₂-2:1 and NiSe₂-CoSe₂-1:2 aerogels toward HER in 1.0M KOH. (b) Tafel slopes of NiSe₂-CoSe₂-300, NiSe₂-CoSe₂-400 and NiSe₂-CoSe₂-500 aerogels toward HER in 1.0M KOH.

Figure S10

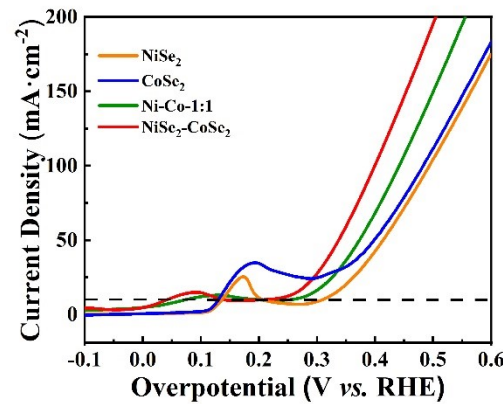


Figure S10. Polarization LSV curves without IR-correction of NiSe_2 , CoSe_2 , Ni-Co, and $\text{NiSe}_2\text{-CoSe}_2$ aerogels toward OER in 1.0M KOH.

Figure S11

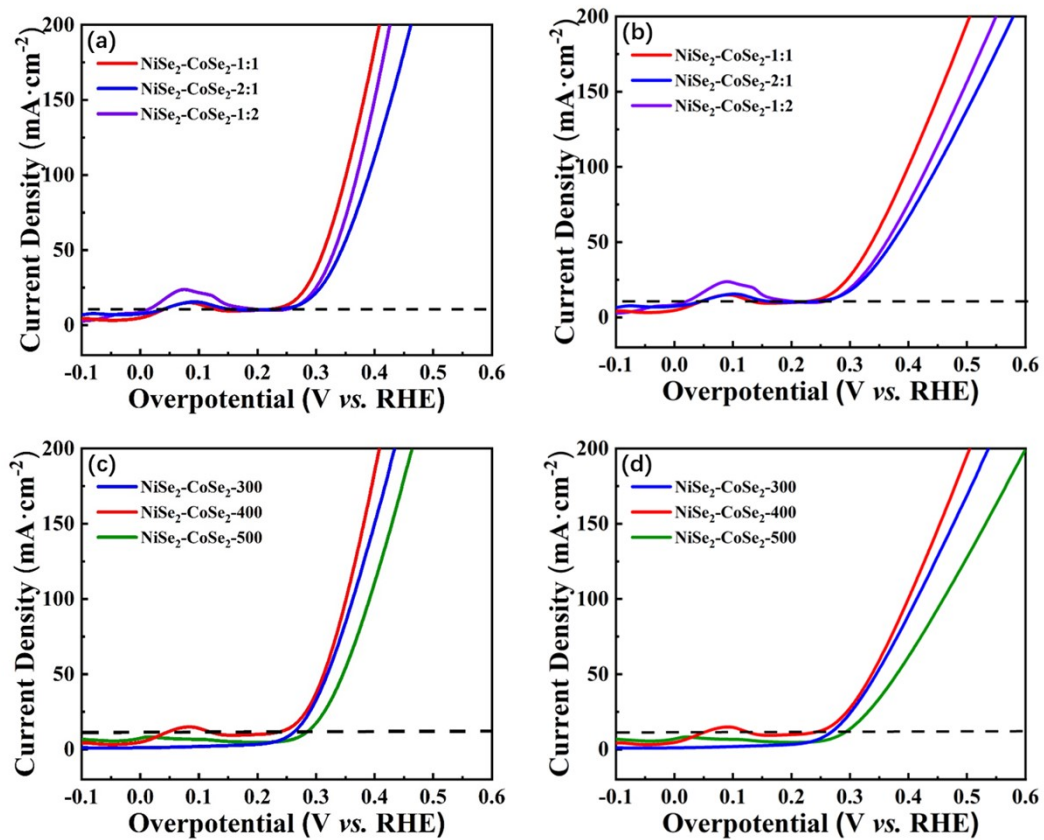


Figure S11. (a-b) Polarization LSV curves of NiSe₂-CoSe₂-1:1, NiSe₂-CoSe₂-2:1 and NiSe₂-CoSe₂-1:2 aerogels toward OER in 1.0M KOH (with and without IR-correction). (c-d) Polarization LSV curves of NiSe₂-CoSe₂-300, NiSe₂-CoSe₂-400 and NiSe₂-CoSe₂-500 aerogels toward OER in 1.0M KOH (with and without IR-correction).

Figure S12

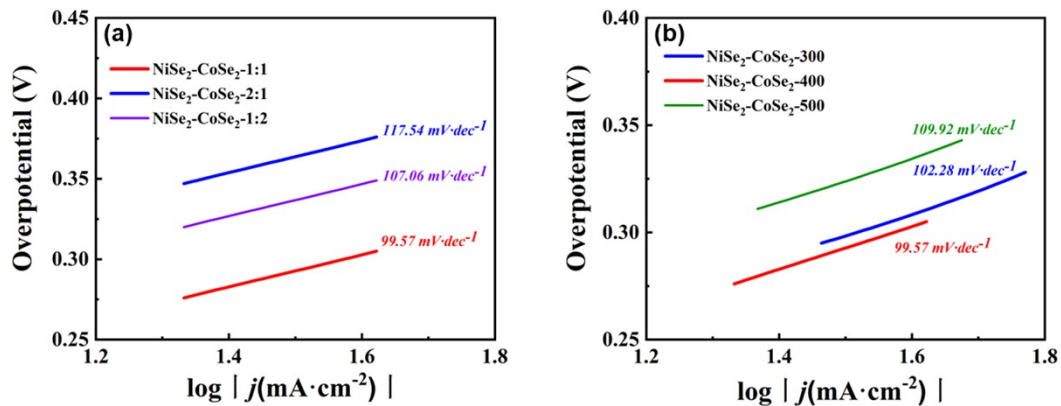


Figure S12. (a) Tafel slopes of NiSe₂-CoSe₂-1:1, NiSe₂-CoSe₂-2:1 and NiSe₂-CoSe₂-1:2 aerogels toward OER in 1.0M KOH. (b) Tafel slopes of NiSe₂-CoSe₂-300, NiSe₂-CoSe₂-400 and NiSe₂-CoSe₂-500 aerogels toward OER in 1.0M KOH.

Figure S13

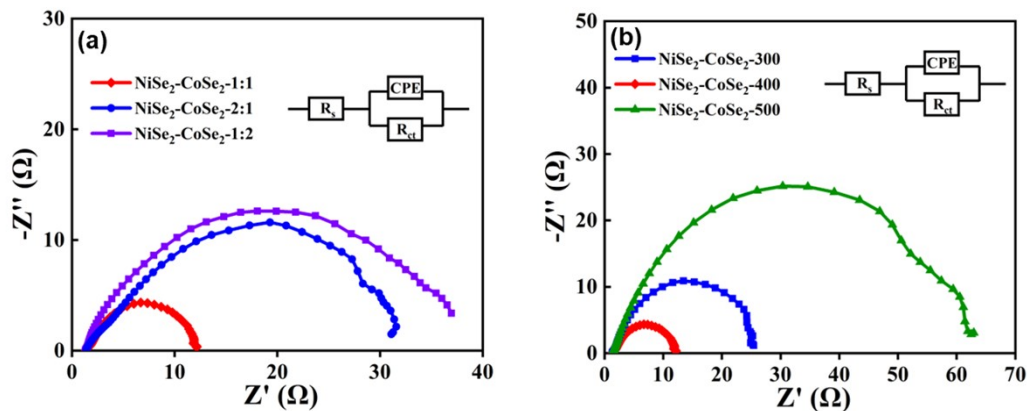


Figure S13. (a) EIS measurements of $\text{NiSe}_2\text{-CoSe}_2$ -1:1, $\text{NiSe}_2\text{-CoSe}_2$ -2:1 and $\text{NiSe}_2\text{-CoSe}_2$ -1:2. (b) EIS measurements of $\text{NiSe}_2\text{-CoSe}_2$ -300, $\text{NiSe}_2\text{-CoSe}_2$ -400 and $\text{NiSe}_2\text{-CoSe}_2$ -500 aerogels.

Figure S14

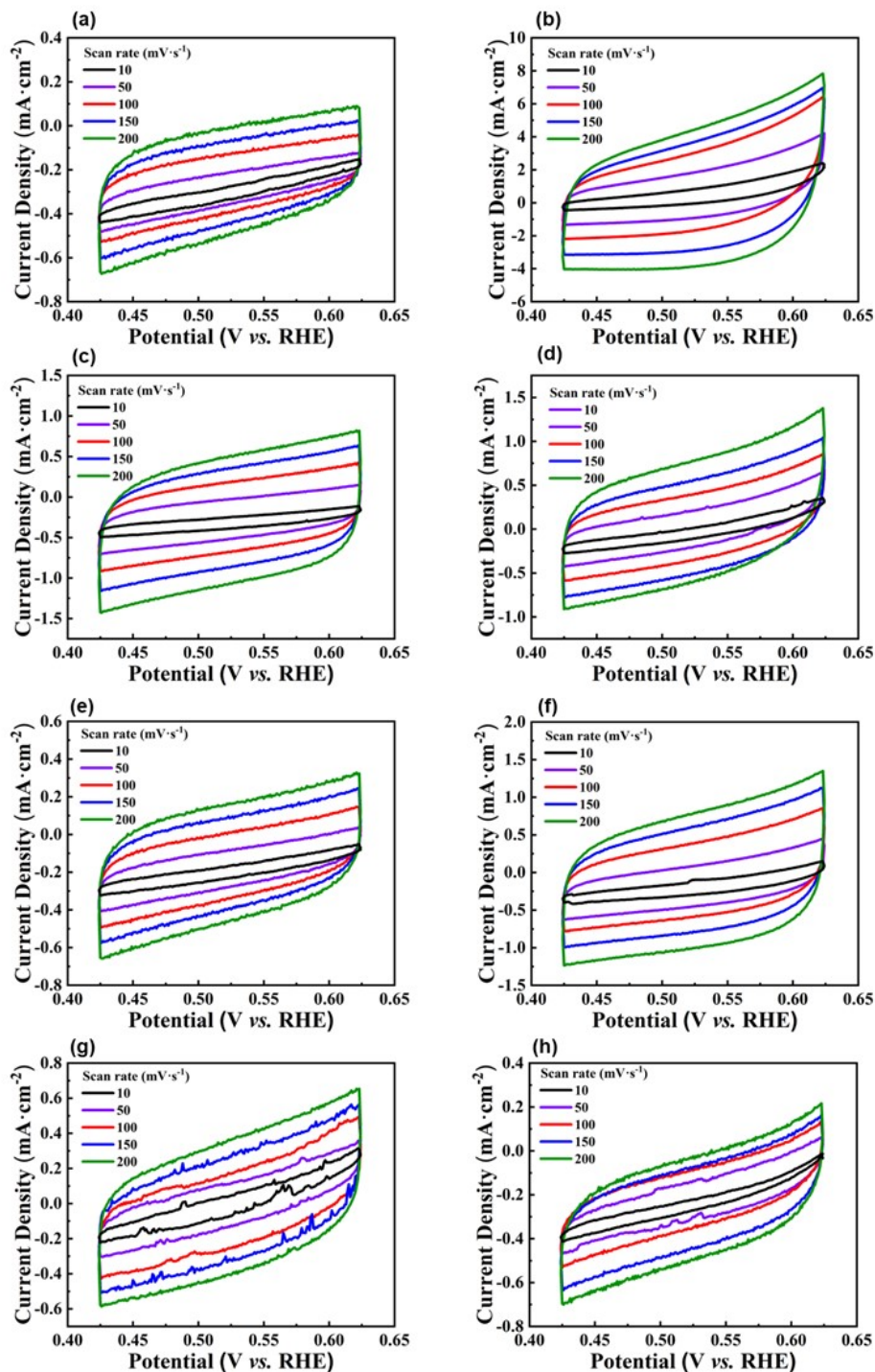


Figure S14. CV curves of all samples: (a) Ni-Co, (b) NiSe₂-CoSe₂, (c) NiSe₂, (d) CoSe₂, (e) NiSe₂-CoSe₂-2:1, (f) NiSe₂-CoSe₂-1:2, (g) NiSe₂-CoSe₂-300, (h) NiSe₂-CoSe₂-500.

Figure S15

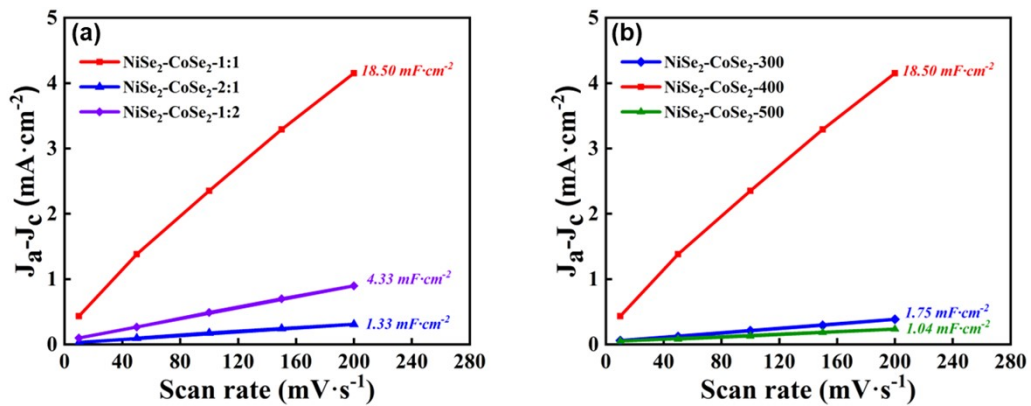


Figure S15. (a) C_{dl} values of $\text{NiSe}_2\text{-CoSe}_2\text{-1:1}$, $\text{NiSe}_2\text{-CoSe}_2\text{-2:1}$ and $\text{NiSe}_2\text{-CoSe}_2\text{-1:2}$.
(b) C_{dl} values of $\text{NiSe}_2\text{-CoSe}_2\text{-300}$, $\text{NiSe}_2\text{-CoSe}_2\text{-400}$ and $\text{NiSe}_2\text{-CoSe}_2\text{-500}$ aerogels.

Figure S16

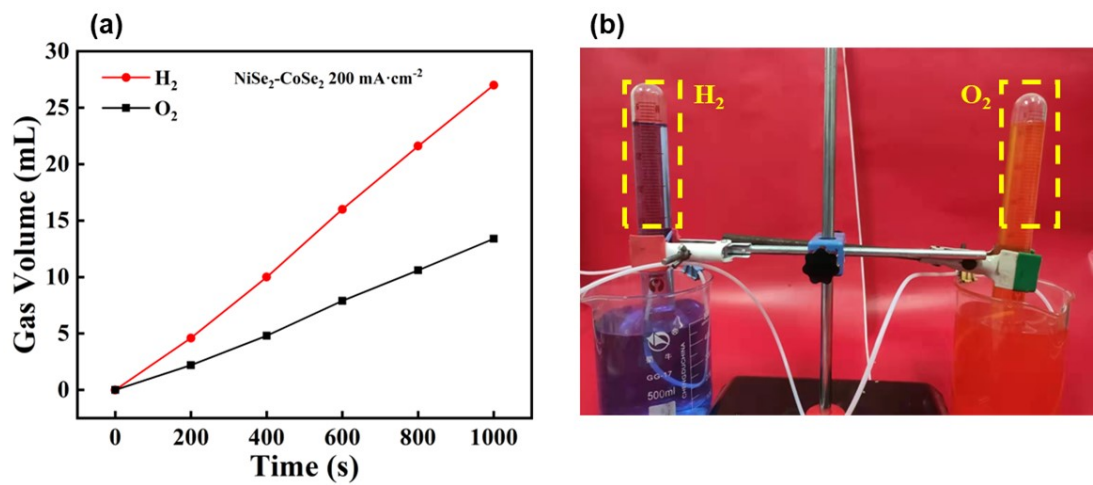


Figure S16. (a) Amounts of gas collected of NiSe₂-CoSe₂ during water splitting, pushing with a current density of 200 mA·cm⁻². (b) Photo of gas collecting device.

Figure S17

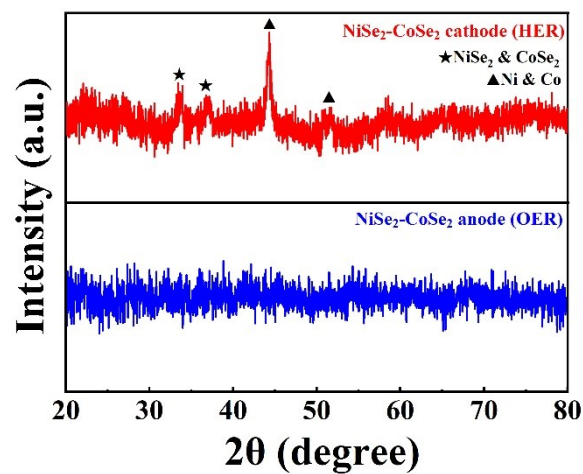


Figure S17. XRD patterns of NiSe₂-CoSe₂ aerogel after the stability test of overall water splitting

Table S1

Table S1. ICP-OES results of SEM-EDS of NiSe₂-CoSe₂-1:1, NiSe₂-CoSe₂-2:1 and NiSe₂-CoSe₂-1:2 aerogels.

Sample	Element	Content (mg/kg)	Mass Fraction (%)
NiSe ₂ -CoSe ₂ -1:1	Ni	287485.64	28.75
	Co	277957.57	27.80
	Se	377840.08	37.78
NiSe ₂ -CoSe ₂ -2:1	Ni	303203.24	30.32
	Co	148425.37	14.84
	Se	364213.43	36.42
NiSe ₂ -CoSe ₂ -1:2	Ni	187144.77	18.71
	Co	353980.56	35.40
	Se	384152.14	38.41

Table S2Table S2. C_{dl} value comparison of $\text{NiSe}_2\text{-CoSe}_2$ aerogel and reported electrocatalysts.

Sample	Morphology	C_{dl} value ($\text{mF}\cdot\text{cm}^{-2}$)
$\text{NiSe}_2\text{-CoSe}_2$ aerogel (This work)	Aerogel	18.50
$\text{CoSe}_2@\text{NiSe}_2/\text{NF}$ [1]	Nanowires array	16.43
$(\text{Ni},\text{Co})\text{Se}_2\text{-GA}$ [2]	Nanocages	16.00
$(\text{Ni}, \text{Co})_{0.85}\text{Se}/\text{NF}$ [3]	Nanosheets array	3.55
$\text{Ni}_2\text{P}-\text{NiSe}_2/\text{CC}$ [4]	Nanosheets and nanoparticles	31.00
$\text{NiSe}_2\text{-Ni}_2\text{P}/\text{NF}$ [5]	Nanowrinkles	39.50

Table S3

Table S3. Performance comparison of NiSe₂-CoSe₂ aerogel and reported electrocatalysts.

Sample	η_{10} of HER (mV)	Tafel slope of HER (mV·dec ⁻¹)	η_{10} of OER (mV)	Tafel slope of OER (mV·dec ⁻¹)	Cell voltage of overall water splitting (V)
NiSe ₂ -CoSe ₂ aerogel (This work)	65	57.54	220	99.57	1.56 (10 mA·cm ⁻²)
(Ni,Co)Se ₂ -GA (Powder)[2]	128	79	250	70	1.60 (10 mA·cm ⁻²)
Ni _{0.2} Co _{0.8} Se (Powder)[6]	73	54.8	280	86.8	1.59 (10 mA·cm ⁻²)
MoCoSe _x @NC (Powder)[7]	60	64	-	-	-
Co _{0.8} Mo _{0.2} Se (Powder)[8]	86.7	58.7	-	-	-
Co _{1.8} Ni(OH) _{5.6} @Co _{1.8} NiS _{0.4} (OH) _{4.8} (Powder)[9]	-	-	274	45	-
CoSe ₂ @NiSe ₂ /NF (Self-supporting)[1]	162	62.84	235 (η_{20})	43.24	1.50 (10 mA·cm ⁻²)
NiSe ₂ -CoSe ₂ /NCF (Self-supporting)[10]	24	24	250	48	1.69 (100 mA·cm ⁻²)

CoS₂-MoS₂/Ti (Self- supporting)[11]	82	59	266	104	1.56 (10 mA·cm ⁻²)
Graphdiyne@NiOx(OH)y/CC (Self- supporting)[12]	154.3	183.80	292.0	98.27	1.54 (10 mA·cm ⁻²)

Reference

- [1] X. Zhang, Y. Ding, G. Wu, X. Du, CoSe₂@NiSe₂ nanoarray as better and efficient electrocatalyst for overall water splitting, *Int. J. Hydrogen Energy.* 45 (2020) 30611–30621. <https://doi.org/10.1016/j.ijhydene.2020.08.096>.
- [2] X. Xu, H. Liang, F. Ming, Z. Qi, Y. Xie, Z. Wang, Prussian Blue Analogues Derived Penroseite (Ni,Co)Se₂ Nanocages Anchored on 3D Graphene Aerogel for Efficient Water Splitting, (2017) 3–8. <https://doi.org/10.1021/acscatal.7b02079>.
- [3] K. Xiao, L. Zhou, M. Shao, M. Wei, Fabrication of (Ni,Co)0.85Se nanosheet arrays derived from layered double hydroxides toward largely enhanced overall water splitting, *J. Mater. Chem. A.* 6 (2018) 7585–7591. <https://doi.org/10.1039/c8ta01067f>.
- [4] C. Liu, T. Gong, J. Zhang, X. Zheng, J. Mao, H. Liu, Y. Li, Q. Hao, Engineering Ni₂P-NiSe₂ heterostructure interface for highly efficient alkaline hydrogen evolution, *Appl. Catal. B Environ.* 262 (2020) 1–8. <https://doi.org/10.1016/j.apcatb.2019.118245>.
- [5] P. Wang, Z. Pu, W. Li, J. Zhu, C. Zhang, Y. Zhao, S. Mu, Coupling NiSe₂-Ni₂P heterostructure nanowrinkles for highly efficient overall water splitting, 377 (2019) 600–608. <https://doi.org/10.1016/j.jcat.2019.08.005>.
- [6] Z. Qian, Y. Chen, Z. Tang, Z. Liu, X. Wang, Hollow Nanocages of - Ni_xCo_{1-x}Se for Efficient Zinc – Air Batteries and Overall Water Splitting, *Nano-Micro Lett.* 11 (2019) 1–17. <https://doi.org/10.1007/s40820-019-0258-0>.
- [7] Y.N. Zhou, Y. Ma, L. Feng, J. Zhao, Z. Tong, B. Dong, Y.R. Zhu, L. Wang, C.G. Liu, Y.M. Chai, Optimized Mo-doped cobalt selenides coupled carbon nanospheres for efficient hydrogen evolution, *Appl. Surf. Sci.* 531 (2020). <https://doi.org/10.1016/j.apsusc.2020.147404>.
- [8] Y. Zhou, J. Zhang, H. Ren, Y. Pan, Y. Yan, F. Sun, X. Wang, S. Wang, J. Zhang, Mo doping induced metallic CoSe for enhanced electrocatalytic hydrogen evolution, *Appl. Catal. B Environ.* 268 (2020) 118467. <https://doi.org/10.1016/j.apcatb.2019.118467>.
- [9] B. Wang, C. Tang, H.F. Wang, X. Chen, R. Cao, Q. Zhang, A Nanosized CoNi Hydroxide@Hydroxysulfide Core–Shell Heterostructure for Enhanced Oxygen Evolution, *Adv. Mater.* 31 (2019) 1–7. <https://doi.org/10.1002/adma.201805658>.
- [10] D. Chen, Z. Xu, W. Chen, G. Chen, J. Huang, J. Huang, C. Song, C. Li, K. (Ken) Ostrikov, Just add water to split water: ultrahigh-performance bifunctional electrocatalysts fabricated using eco-friendly heterointerfacing of NiCo diselenides, *J. Mater. Chem. A.* 8 (2020) 12035–12044. <https://doi.org/10.1039/d0ta02121k>.
- [11] Y. Li, W. Wang, B. Huang, Z. Mao, R. Wang, B. He, Y. Gong, H. Wang, Abundant heterointerfaces in MOF-derived hollow CoS₂–MoS₂ nanosheet array electrocatalysts for overall water splitting, *J. Energy Chem.* 57 (2021) 99–108. <https://doi.org/10.1016/j.jechem.2020.08.064>.
- [12] C. Zhang, Y. Xue, L. Hui, Y. Fang, Y. Liu, Y. Li, Graphdiyne@NiOx(OH)heterostructure for efficient overall water splitting, *Mater. Chem. Front.* 5 (2021) 5305–5311. <https://doi.org/10.1039/d1qm00466b>.